

Supporting Information for

**Salt-bridge mediated cooperativity and mechanical stabilization of
tandem spectrin repeats**

Text S1. Plasmid constructs and protein expression.

1. Detailed sequences of Avi-(ACTN1-SR3-SR4)-Spy:

MHHHHHHGKPIPNNLLGLDSTENLYFQGIDPFTGLNDIFEAQKIEWHEGGGSG
KLTEKLLLETIDQLYLEYAKRAAPFNNWMEGAMEDLQDTFIVHTIEEIQGLTTA
HEQFKATLPDADKERLAILGIHNEVSKIVQTYHVN MAGTNPYTTITPQEINGK
WDHVRQLVPRRDQALTEEHARQQHNERLRKQFGAQANVIGPWIQTKMEEIG
RISIEMHGTLEDQLSHLRQYEKSIVNYKPKIDQLEGDHQLIQEALIFDNKHTNY
TMEHIRVGWEQLLTTIARTINEVENQILTRDAKGISQEFGGGSGAHIVMVDAY
KPTK*

The colored sequence is the 500th-745th a.a. residues based on the human alpha-actinin 1 (Uniprot P12814). The red colored sequence is the linker between SR3 and SR4. The two orange colored sequences are linkers between SR2 and SR3, SR4 and EF hand, respectively.

2. Detailed sequences of Avi-(ACTN1-SR4)₆-Spy:

MHHHHHHGKPIPNNLLGLDSTENLYFQGIDPFTGLNDIFEAQKIEWHEGFEDK
VWYDLDAKLGDIKFNKGGGSGLEEHARQQHNERLRKQFGAQANVIGPW
IQTKMEEIGRISIEMHGTLEDQLSHLRQYEKSIVNYKPKIDQLEGDHQLIQEALI
FDNKHTNYTMEHIRVGWEQLLTTIARTINEVENQILTRDAKGISQGGGSGEHA
RQQHNERLRKQFGAQANVIGPWIQTKMEEIGRISIEMHGTLEDQLSHLRQYE
KSIVNYKPKIDQLEGDHQLIQEALIFDNKHTNYTMEHIRVGWEQLLTTIARTIN
EVENQILTRDAKGISQGGGSGEHAHQHNERLRKQFGAQANVIGPWIQTKME

EIGRISIEMHGTLEDQLSHLRQYEKSIVNYKPKIDQLEGDHQLIQEALIFDNKH
TNYTMEHIRVGWEQLLTTIARTINEVENQILTRDAKGISQGGGSGEHARQQHN
ERLRKQFGAQANVIGPWIQTKMEEIGRISIEMHGTLEDQLSHLRQYEKSIVNY
KPKIDQLEGDHQLIQEALIFDNKHTNYTMEHIRVGWEQLLTTIARTINEVENQI
LTRDAKGISQGGGSGEHARQQHNERLRKQFGAQANVIGPWIQTKMEEIGRISI
EMHGTLEDQLSHLRQYEKSIVNYKPKIDQLEGDHQLIQEALIFDNKHTNYTM
EHIRVGWEQLLTTIARTINEVENQILTRDAKGISQGGGSGEHARQQHNERLRK
QFGAQANVIGPWIQTKMEEIGRISIEMHGTLEDQLSHLRQYEKSIVNYKPKID
QLEGDHQLIQEALIFDNKHTNYTMEHIRVGWEQLLTTIARTINEVENQILTRDA
KGISQGGGSGAHIVMVDAYKPTK*

Text S2. Transition step size to residue number conversion.

The force-extension curve of SR3/SR4/SR34 is determined by the rigid rotation fluctuation of a characteristic rigid-body with a length $b \sim 4.5$ nm, estimated from the PDB file of the folded domain, which is the distance between the two force-attaching points (i.e., the N- to C- terminal distance in our experiment). This force-extension curve can be described by the freely-jointed chain polymer model with a single segment:

$$x^{\text{FJC}}(f) = b \left(\coth \left(\frac{fb}{k_{\text{B}}T} \right) - \frac{k_{\text{B}}T}{fb} \right). \quad (\text{S1})$$

The unfolded state of a domain can be a flexible peptide chain, and this force-extension curve can be described by the worm-like chain (WLC) polymer model through the Marko-Siggia formula¹ with a bending persistence length of $A \sim 0.8$ nm:

$$\frac{fA}{k_{\text{B}}T} = \frac{1}{4 \left(1 - \frac{x^{\text{WLC}}(f)}{l} \right)^2} - \frac{1}{4} + \frac{x^{\text{WLC}}(f)}{l}, \quad (\text{S2})$$

where $l = n * l_0$ is the contour length of the unfolded domain, n is the number of residues of the domain, $l_0 = 0.38$ nm is the contour length of per residue. Hence the unfolding/refolding step-size is the extension differences of the domain before and after unfolding at the transition (unfolding/refolding) force, i.e.,

$$\Delta x(f) = x^{\text{WLC}}(f) - x^{\text{FJC}}(f). \quad (\text{S3})$$

Based on the above equations, the contour length l and the number of residues n involved in the transition can be obtained from the measured step-sizes of the transition at given force.

α actinin-1 SR3-SR4 predicted by AlphaFold3

α actinin-2 SR3-SR4 PDB ID :1SJJ

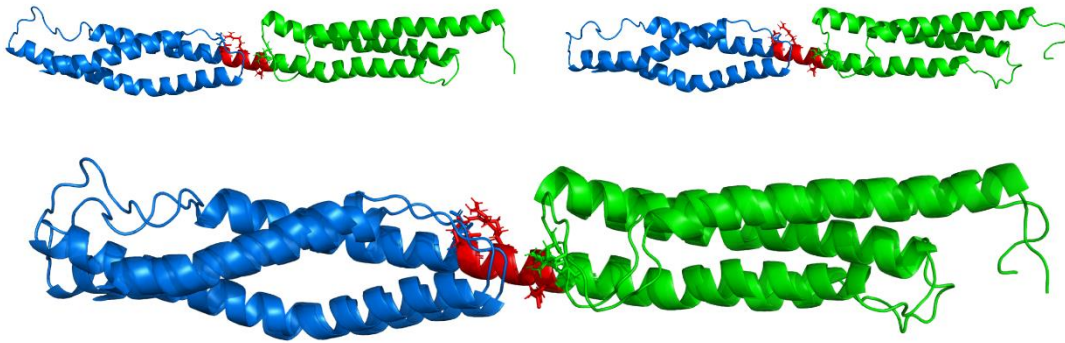


Figure S1. Comparison of the α actinin-1 SR34 structure predicted by AlphaFold3 with the α actinin-2 SR34 structure (PDB ID: 1SJJ) from the PDB database. All structures were equilibrated by 100 ns relaxation simulation.

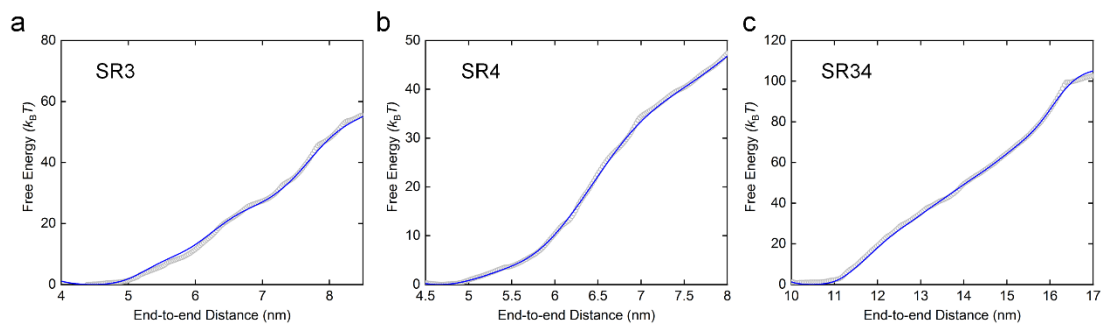


Figure S2. Free energy versus end-to-end distance profiles for (a) SR3, (b) SR4 and (c) SR34, respectively. Discrete data (gray circles) obtained from WHAM umbrella sampling analysis, in consistent with the blue curves which obtained by integrating the force with respect to the end-to-end distance of protein in Figure 5a to 5c.

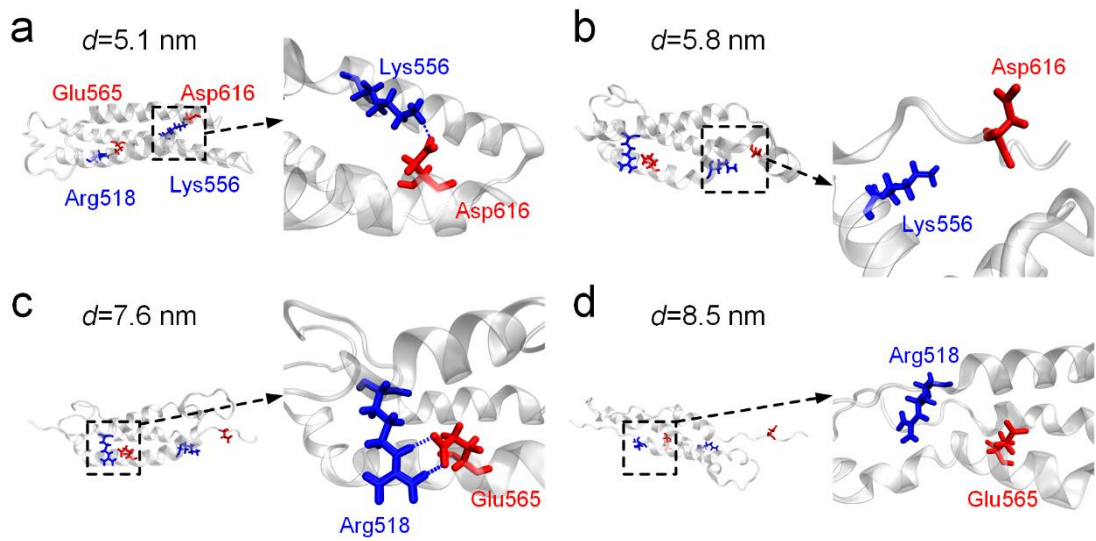


Figure S3. Representative structures for SR3 at the end-to-end distance of (a) $d = 5.1$ nm, (b) $d = 5.8$ nm, (c) $d = 7.6$ nm and (d) $d = 8.5$ nm. Representative amino acid residues are colored according to positively/negatively charged. Salt bridges Lys556-Asp616 and Arg518-Glu565 are abolished during the stretching of SR3, in consistent with the curve peaks in Figure 5a.

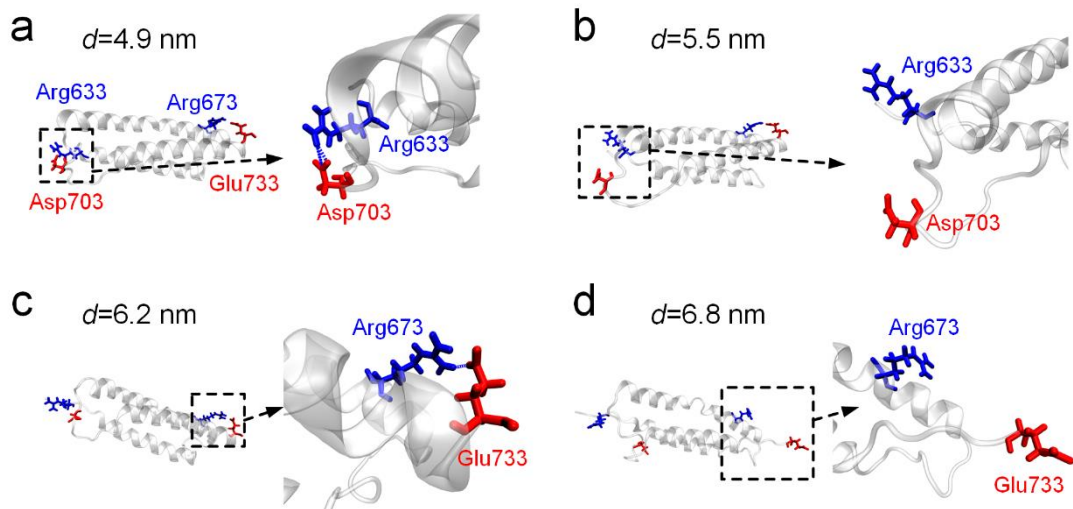


Figure S4. Representative structures for SR4 at the end-to-end distance of (a) $d = 4.9$ nm, (b) $d = 5.5$ nm, (c) $d = 6.2$ nm and (d) $d = 6.8$ nm. Salt bridges Arg633-Asp703 and Arg673-Glu733 are abolished during the stretching of SR4, in consistent with the curve peaks in Figure 5b.

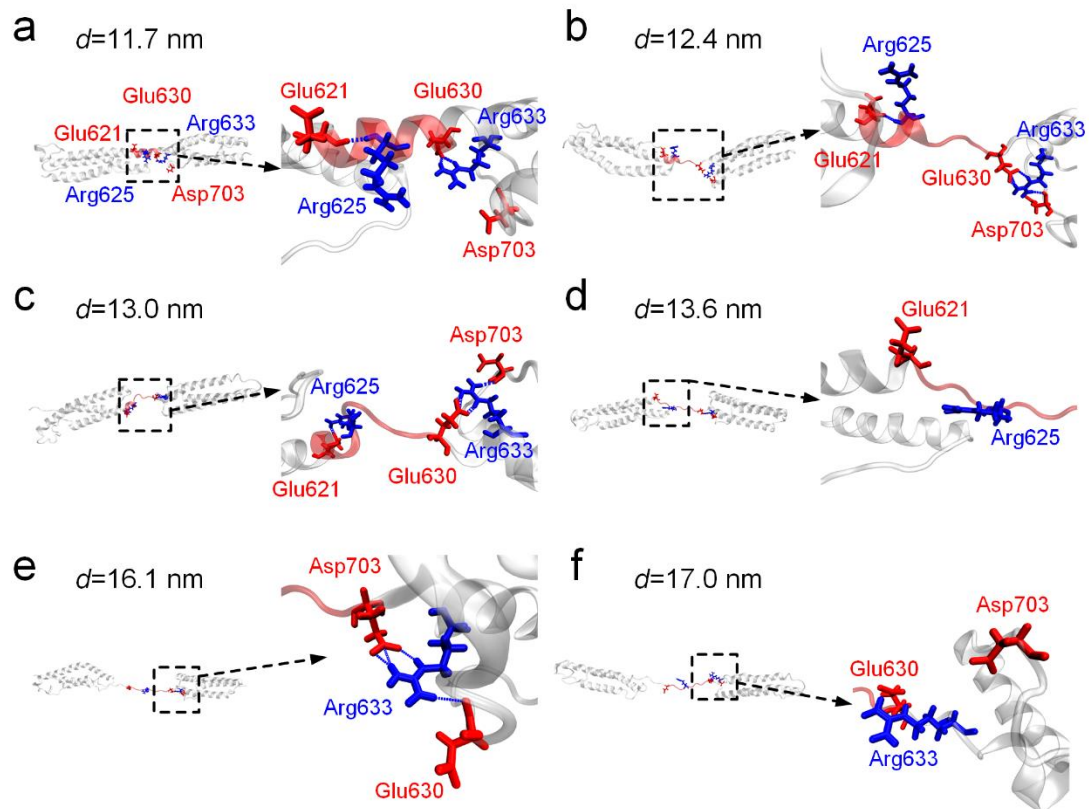


Figure S5. Representative structures for SR34 at the end-to-end distance of (a) $d = 11.7$ nm, (b) $d = 12.4$ nm, (c) $d = 13.0$ nm, (d) $d = 13.6$ nm, (e) $d = 16.1$ nm and (f) $d = 17.0$ nm. The α -helical linker partially unwind (residues 627 to 633) at a $d = 12.4$ nm, and salt bridges Glu621-Arg625, Glu630-Asp703 and Arg633-Asp703 are abolished during the stretching of SR34, in consistent with the curve peaks in Figure 5c.

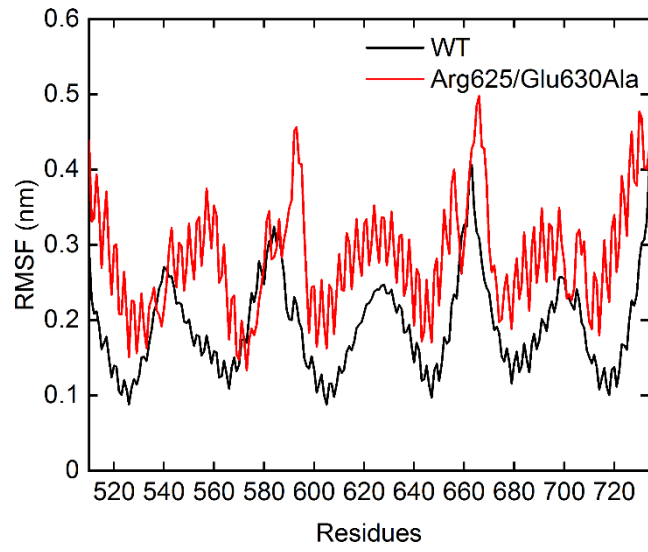


Figure S6. Root-mean-square-fluctuation (RMSF) of wild type (black) and mutant (red) of SR34 computed for the backbone atoms are shown as a function of residue number.

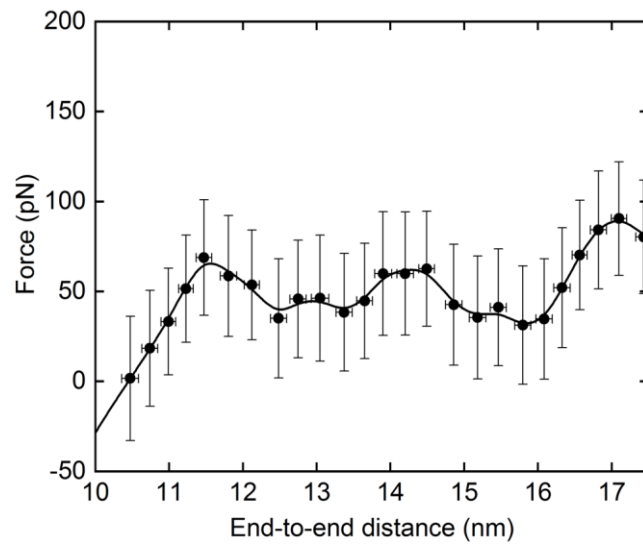


Figure S7. The force-distance relation of SR34 with point mutations for Arg625/Glu630Ala.

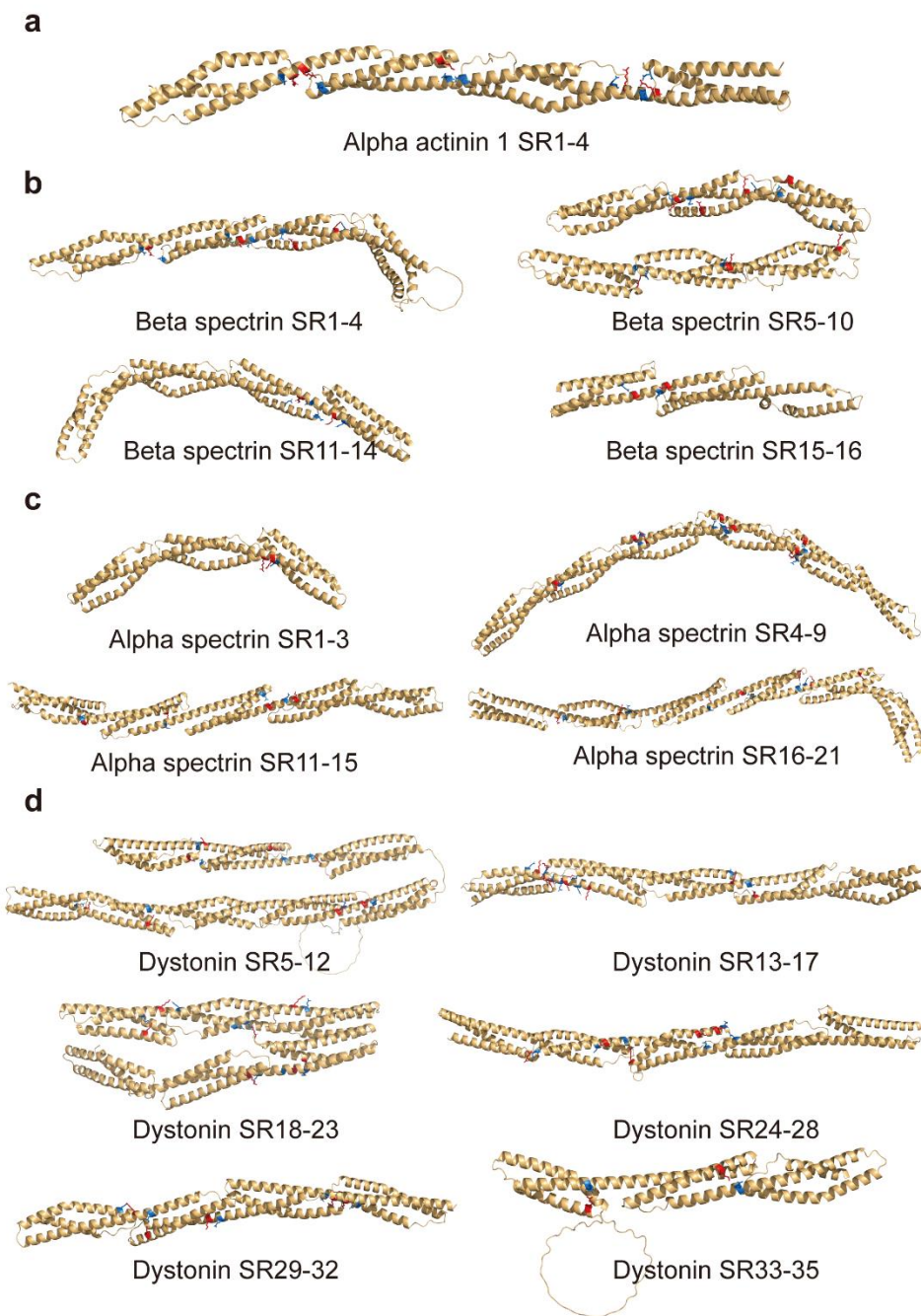


Figure S8. The AlphaFold predicted SR structures of spectrin superfamily proteins. (a-d) The AlphaFold predicted SR structures of alpha-actinin 1 (a), beta-spectrin (b), alpha spectrin (c), and dystonin (d). The potential linker-mediated salt-bridge are highlighted with red (Arg, His, and Lys) and blue (Asp and Glu) colors. The potential formation of salt-bridge is determined based on the measured distance (<0.5 nm) between the salt bridge formation residues.

- (1) Marko, J. F.; Siggia, E. D. Stretching DNA. *Macromolecules* **1995**, *28* (26), 8759–8770.
- (2) Chen, H.; Fu, H.; Zhu, X.; Cong, P.; Nakamura, F.; Yan, J. Improved High-Force Magnetic Tweezers for Stretching and Refolding of Proteins and Short DNA. *Biophysical Journal* **2011**, *100* (2), 517–523.
- (3) Le, S.; Liu, R.; Lim, C. T.; Yan, J. Uncovering Mechanosensing Mechanisms at the Single Protein Level Using Magnetic Tweezers. *Methods* **2016**, *94*, 13–18.
- (4) Le, S.; Yao, M.; Chen, J.; Efremov, A. K.; Azimi, S.; Yan, J. Disturbance-Free Rapid Solution Exchange for Magnetic Tweezers Single-Molecule Studies. *Nucleic Acids Res* **2015**, *43* (17), e113–e113.
- (5) Le, S.; Yu, M.; Yan, J. Phosphorylation Reduces the Mechanical Stability of the α -Catenin/ β -Catenin Complex. *Angew Chem Int Ed* **2019**, *58* (51), 18663–18669.
- (6) Le, S.; Hu, X.; Yao, M.; Chen, H.; Yu, M.; Xu, X.; Nakazawa, N.; Margadant, F. M.; Sheetz, M. P.; Yan, J. Mechanotransmission and Mechanosensing of Human Alpha-Actinin 1. *Cell Reports* **2017**, *21* (10), 2714–2723.
- (7) Le, S.; Yu, M.; Hovan, L.; Zhao, Z.; Ervasti, J.; Yan, J. Dystrophin As a Molecular Shock Absorber. *ACS Nano* **2018**, *12* (12), 12140–12148.
- (8) Van Der Spoel, D.; Lindahl, E.; Hess, B.; Groenhof, G.; Mark, A. E.; Berendsen, H. J. C. GROMACS: Fast, Flexible, and Free. *J Comput Chem* **2005**, *26* (16), 1701–1718.
- (9) Jorgensen, W. L.; Chandrasekhar, J.; Madura, J. D.; Impey, R. W.; Klein, M. L. Comparison of Simple Potential Functions for Simulating Liquid Water. *The Journal of Chemical Physics* **1983**, *79* (2), 926–935.
- (10) Lindorff-Larsen, K.; Piana, S.; Palmo, K.; Maragakis, P.; Klepeis, J. L.; Dror, R. O.; Shaw, D. E. Improved Side-chain Torsion Potentials for the Amber ff99SB Protein Force Field. *Proteins* **2010**, *78* (8), 1950–1958.
- (11) Liu, J.; Taylor, D. W.; Taylor, K. A. A 3-D Reconstruction of Smooth Muscle α -Actinin by CryoEm Reveals Two Different Conformations at the Actin-Binding Region. *Journal of Molecular Biology* **2004**, *338* (1), 115–125.
- (12) Hoover, W. G. Canonical Dynamics: Equilibrium Phase-Space Distributions. *Phys. Rev. A* **1985**, *31* (3), 1695–1697.
- (13) Parrinello, M.; Rahman, A. Polymorphic Transitions in Single Crystals: A New Molecular

Dynamics Method. *Journal of Applied Physics* **1981**, 52 (12), 7182–7190.

(14) Darden, T.; York, D.; Pedersen, L. Particle Mesh Ewald: An $N \cdot \log(N)$ Method for Ewald Sums in Large Systems. *The Journal of Chemical Physics* **1993**, 98 (12), 10089–10092.

(15) Hess, B. P-LINCS: A Parallel Linear Constraint Solver for Molecular Simulation. *J. Chem. Theory Comput.* **2008**, 4 (1), 116–122.

(16) Kumar, S.; Rosenberg, J. M.; Bouzida, D.; Swendsen, R. H.; Kollman, P. A. THE Weighted Histogram Analysis Method for Free-energy Calculations on Biomolecules. I. The Method. *J Comput Chem* **1992**, 13 (8), 1011–1021.

(17) Cong, P.; Dai, L.; Chen, H.; van der Maarel, J. R. C.; Doyle, P. S.; Yan, J. Revisiting the Anomalous Bending Elasticity of Sharply Bent DNA. *Biophysical Journal* **2015**, 109 (11), 2338–2351.